Available online at www.sciencedirect.com
SCIENCE DIRECT®
Journal of Non-Crystalline Solids 350 (2004) 152–164
JOURNAL OF NON-CRYSTALLINE SOLIDS
www.elsevier.com/locate/jnoncrysol

Isocyanate-crosslinked silica aerogel monoliths: preparation and characterization

Guohui Zhang [a], Amala Dass [a], Abdel-Monem M. Rawashdeh [a], Jeffery Thomas [a], Joseph A. Counsil [a], Chariklia Sotiriou-Leventis [a,*], Eve F. Fabrizio [b,1], Faysal Ilhan [b,1], Plousia Vassilaras [b,2], Daniel A. Scheiman [b,3], Linda McCorkle [b,1], Anna Palczer [b], J. Chris Johnston [b], Mary Ann Meador [b], Nicholas Leventis [b,*]

[a] *Department of Chemistry, University of Missouri-Rolla, Rolla, MO 65409, United States*
[b] *NASA Glenn Research Center, Materials Division, 21000, Brookpark Road, M.S. 49-1, Cleveland, OH 44135, United States*

Available online 6 November 2004

Abstract

Polymerization of di- and tri-isocyanates can be templated onto the mesoporous surface of a preformed network of sol–gel-derived silica nanoparticles, resulting in a conformal 'crosslinked' coating that renders the interparticle neck zone wider. Upon drying, these crosslinked networks yield aerogels which are up to ~3× more dense than native aerogels based on the underlying silica framework, but also up to 10× less hygroscopic and they may take more than 300× the force to break. These results have been obtained with one-step based-catalyzed sol–gel silica networks, as well as with gels derived through a two-step process involving an acid-catalyzed sol and a based-catalyzed gel. Furthermore, it has been also found that crosslinking increases the dielectric constant only by ~35% relative to values reported in the literature for native silica aerogels of about the same porosity. Chemical investigations into the polymerization reaction have shown that the process of crosslinking involves reaction of the isocyanate with: (a) —OH groups at the surface of silica to form carbamate; and (b) adsorbed water, to form an amine and carbon dioxide. This amine then reacts with additional isocyanates resulting in polymer chain extension and bridging of particles with urethane-terminated polyurea.

PACS: 81.05.Qk; 81.05.Rm; 81.05.Zx; 81.07.−b; 81.20.Fw; 81.40.Tv; 82.35.Np

1. Introduction

Nanostructured materials possess macroscopic properties, which are derived from the size and architecture of their constituents at the nanoscopic level [1]. For example, it is known that small amounts of nanoscopic additives to certain plastics improve product performance [2]. Furthermore, if the elementary building blocks of the matrix and the additive are sized similarly, there may be some additional advantages as well, as for example in catalysis [3]. In this context, we have reasoned that if the amounts of the filler and the matrix are about equal, their roles can be reversed and certain desirable properties of the nanostructured filler could be improved selectively.

One common inexpensive additive for plastics is silica. One nanoparticulate form of silica is obtained via the sol–gel process and its most lightweight bulk form

* Corresponding authors. Tel.: +1 573 341 4353 (C. Sotiriou-Leventis), +1 216 433 3202 (N. Leventis).
E-mail addresses: cslevent@umr.edu (C. Sotiriou-Leventis), nicholas.leventis@nasa.gov (N. Leventis).
[1] Employed by Ohio Aerospace Institute.
[2] Summer Intern, 2003.
[3] Employed by QSS Group, Inc.

0022-3093/$ - see front matter © 2004 Elsevier B.V. All rights reserved.
doi:10.1016/j.jnoncrysol.2004.06.041

is the silica aerogel with densities in the range $3\,mg\,cm^{-3}$ to $0.8\,g\,cm^{-3}$ [4–7]. Due to the attributes associated with low density, silica aerogels are ideal materials for a variety of thermal, optical, electronic and chemical applications [8]. However, silica aerogels are also fragile and environmentally unstable materials (e.g., hygroscopic), thus their practical use is limited to specialized environments, for example as Čerenkov radiation detectors in certain nuclear reactors and as thermal insulators in space vehicles such as the Sojourner Rover on Mars in 1997 and the two Mars Exploration Rovers, Spirit and Opportunity, in 2004.

The desirable properties of silica aerogels (low density, low thermal conductivity, and low dielectric constant) stem from the significant amount of mesoporosity (see dark areas in Fig. 1(a)) rendering the bulk mostly empty space filled with air. For example, it can be calculated based on the skeletal density of compact silica (see Section 3.2.1) that the bulk of a typical silica aerogel with a density of $0.1\,g\,cm^{-3}$ consists of ~95% empty space. The bead-like structures forming the 'pearl-necklace' network in Fig. 1(a) are the so-called 'secondary' particles and consist of smaller 'primary' particles of compact silica (refer to Fig. 1(b)). When a silica aerogel monolith breaks under force, only secondary particles lose contact with one another, while the primary particles remain undisturbed. Therefore, by adding a material conformally to the secondary particles, the bulk structure of the silica aerogel network would be reinforced while the mesoporous space between these particles would be maintained. In order to accomplish this reinforcement, an interparticle crosslinker should react with and accumulate only at the surface of silica. In this context, since silica particles are at least partially surface-terminated with —Si—OH groups, it was deemed reasonable to borrow chemistry from polyurethane polymers, letting surface silanols react with a di- and a tri-isocyanate [9]. In polyurethane chemistry, a di- or a tri-isocyanate reacts with a polyol, yielding a polymer via formation of carbamates, Eq. (1). For our purposes, we have replaced the polyol with the preformed silica network, whose surface now plays that role.

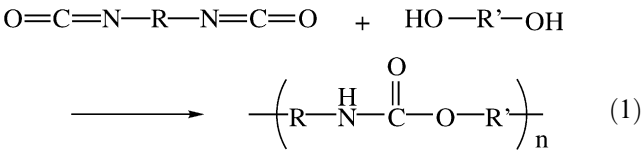

(1)

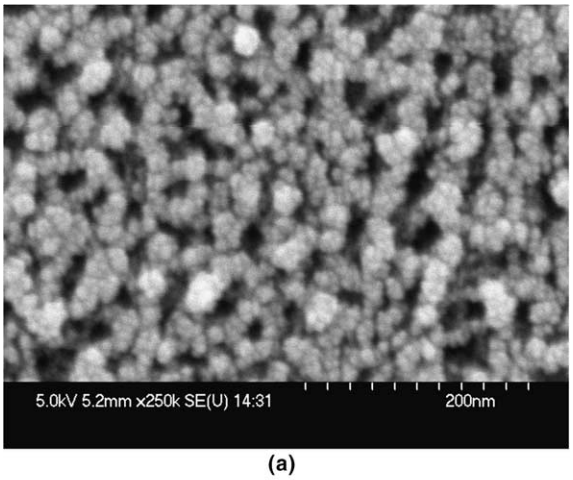

Fig. 1. (a) SEM imaging in the interior of a fractured native silica aerogel monolith with $\rho_b = 0.18\,g\,cm^{-3}$. (b) Nanostructure of mesoporous silica.

2. Experimental

2.1. Materials

All solvents and reagents were used as received from each manufacturer. The isocyanates Desmodur N3200, N3300A, and TDI were obtained courtesy of Bayer Corporation (Pittsburgh, PA). Tetramethoxysilane (TMOS), ammonium hydroxide reagent grade and methanol HPLC grade were purchased from Sigma Aldrich. Absolute ethanol (200 Proof) was from Aaper Alcohol and Chemical Co. Propylene carbonate, reagent grade; acetonitrile, 'Optimum' grade; and, nitric acid, reagent grade, were obtained from Fisher Scientific. Reagent grade acetone was obtained from Spectrum Chemical Co. Deionized water was obtained from a Milli-Q water system supplied by Millipore. Liquid carbon dioxide (gas tank with siphon tube) used for drying was obtained from AGA, Inc. (Cleveland, OH).

2.2. Preparation of wet gels

Native silica wet gels (prior to crosslinking) were prepared using two different methods. One group of silica

wet gels, which are referred to as the one-step gels, were prepared directly from TMOS via a base-catalyzed route [10]. The second set of gels, which are referred to as the two-step gels, were prepared via a modification of a procedure similar to the one described by Tillotson and Hrubesh [11].

In our case, the sol for the two-step wet gels was prepared by mixing together 250 ml of TMOS, 156 ml of absolute ethanol, 63 ml of deionized water and 0.065 ml of nitric acid (molar ratios, TMOS:EtOH:H_2O:HNO_3 = 1:1.5:2:6×10^{-4}). The solution was refluxed for 4 h with stirring. The temperature, which was monitored during this step, remained around the boiling point of ethanol, 78 °C. Next, 250 ml of solvent was distilled off until the temperature of the solution reached ~85 °C. This took ~1 h and 45 min. Once the solution cooled to room temperature, an additional 250 ml of TMOS was added and the solution was refluxed for another 4 h. A second distillation was performed for 45 min until another 110 ml of solvent was removed. Once the viscous solution cooled to room temperature, 215 ml of acetonitrile was added to make up the stock solution used to form gels. The sol and the resulting wet silica gels were prepared through a base-catalyzed reaction by mixing together 5.5 ml of acetonitrile, 0.133 ml of deionized water, 0.013 ml of ammonium hydroxide and then adding either 0.5 ml, 1 ml or 2 ml of the stock solution (8%, 15% and 26% v/v of the total volume, respectively), followed by vigorous mixing.

Monoliths were prepared by pouring the sol solutions into polypropylene molds (Wheaton Polypropylene Omni-Vials, Part No. 225402). Gelation by both the one-step and the two-step methods took ~20 min. One-step wet gels were allowed to age for 48 h, but it was also found that aging does not play any significant role in the strength of crosslinked aerogels; thus, two-step gels were aged for only 2 h before being removed from the molds. For one-step gels, the monoliths were washed with methanol (4×, ~12 h each time) and then with the crosslinking solvent, propylene carbonate or acetone (4×, ~12 h each time). For two-step gels, the monoliths were washed with acetonitrile and then with acetone (4× for each solvent, ~12 h each time).

2.3. Preparation of isocyanate-crosslinked aerogels

Weight percent solutions varying from ~5% to ~55% of each of the isocyanates, Desmodur N3200, N3300A, and TDI, were prepared. In the case of the one-step wet gels, these solutions were prepared in either propylene carbonate or acetone. For the two-step wet gels, these solutions were prepared in either acetonitrile or acetone. When acetonitrile was used as the crosslinking solvent, the additional solvent exchange step into acetone could be eliminated. The isocyanate crosslinkers were allowed to diffuse from the solution into the wet gels and to equilibrate for 24 h. The crosslinking temperature was 95 °C for propylene carbonate, 80 °C for acetonitrile and 52 °C for acetone, samples typically remaining in the oven for 72 h. After heating, samples were cooled to room temperature, the crosslinking solution was decanted, and samples from propylene carbonate- or acetone-based crosslinking solutions were washed with acetone (4×, 12 h each time). Two-step samples from acetonitrile-based crosslinking solutions were washed either with acetonitrile or acetone. After the final wash cycle, samples were transferred into an autoclave (SPI-DRY Jumbo Supercritical Point Drier, SPI Supplies, Inc., West Chester, PA) and dried with CO_2 taken out supercritically.

2.4. Preparation of samples for control experiments

In order to determine the spectroscopic characteristics of carbamate, a product resulting from the reaction of isocyanate with a hydroxyl group, two monomers, Desmodur N3200 and Desmodur N3300A, were reacted for 24 h with methanol at room temperature using methanol as the solvent. At the end of this time period, the solvent was removed under reduced pressure and the oily product was characterized by infrared and ^{13}C-NMR spectroscopies. Similarly, in order to determine the spectroscopic characteristics of urea, a product resulting from the reaction of isocyanate with an amine, the same two isocyanates were reacted for 24 h at room temperature with isopropylamine, using isopropylamine as solvent. Both reactions gave solid products that were filtered off and washed with acetone. Similarly, a reaction with water in an acetone solution gave a solid product and carbon dioxide. Exposure of a thin liquid layer of N3200 to the ambient environment for ~1 week gave a hard, compact, clear solid material that was spectroscopically (infrared and ^{13}C-NMR) identical to the solid product of the reaction of N3200 with water. The density of this material (N3200-derived polyurea) was characterized gravimetrically according to ASTM D3171-76 Procedure B, and found to be $1.144 \pm 0.001\,g\,cm^{-3}$.

2.5. Methods

Chemical characterization of crosslinked aerogel monoliths and of all control samples was conducted by infrared and ^{13}C-NMR spectroscopy. All solid samples were ground by ball-milling for 5 min using a SPEX 5300 Mixer Mill (SPEX Inc., Edison, NJ). Infrared spectra were obtained with a Nicolet-FTIR Spectrometer Model 750. Liquid samples were run neat between NaCl plates; solid samples were mixed with KBr and pressed into a pellet. The solution NMR spectra were obtained with a Varian Unity Inova 400 Widebore NMR instrument using a variable temperature 10 mm multinuclear liquids probe. Standard single-pulse ^{1}H and ^{13}C pulse

sequences were used. Solid ^{13}C-NMR spectra were obtained on a Bruker Avance 300 Spectrometer, using cross-polarization and magic-angle spinning at 7 kHz. The acquisition also employed spinning-sideband suppression using a TOSS sequence. The spectra were externally referenced to the carbonyl of glycine (196.1 relative to tetramethylsilane, TMS).

Monomers (Desmodur N3200 and Desmodur N3300A) were also characterized by liquid chromatography–mass spectrometry (LC–MS) using a Waters Alliance 2690 pump interfaced with a 996 Photodiode Array detector (200–400 nm) and a Finnigan LCQ (ESI, 100–1500 AMU) mass spectrometer. A flow rate of 1 $cm^3 min^{-1}$ was used with a solvent gradient of 25% acetonitrile and 75% water to 100% acetonitrile over 40 min. The column was a Hamilton PRP-1 (10 μm, 75Å, polystyrene divinylbenzene, 4.1 mm ID × 250 mm).

Carbon dioxide was identified as byproduct of the crosslinking process using a Nicolet 510P FTIR spectrometer. For this purpose a typical one-step wet gel was placed in a crosslinking solution consisting of 55% w/w of Desmodour N3200 in acetone and allowed to crosslink for 3 d at 53 °C in a sealed container with a septum port. In a control experiment, an equal volume of the crosslinking solution was heated without a gel in a similar container. A gas-tight syringe was used to sample the headspace gases. A Pyrex™ 100 cm^3 gas cell with KBr windows and septum ports was purged with dry nitrogen and was used to record the FTIR spectrum. The background was measured with the gas cell and the FTIR cell compartment filled with dry nitrogen. The sample (10 cm^3) was then injected into the gas cell, and the spectrum was recorded. A second background was taken with the gas cell filled with ambient air. The control did not give any absorption above what is given by the gas cell filled with air. The sample gave 13 times stronger absorption than the control.

Physical characterization of native and crosslinked silica aerogel samples was conducted by thermogravimetric analysis (TGA), NMR imaging, scanning electron microscopy (SEM), nitrogen-adsorption porosimetry, three-point flexural bending and dielectric testing. The TGA was performed using a TA Instruments Model 2950 HiRes instrument. Samples were run at a temperature ramp rate of 10 °C min^{-1} under nitrogen or air. The NMR imaging was conducted on a Varian Unity Inova 400 Widebore NMR Spectrometer with the 25 mm coil in the microimaging system. Proton images were acquired using the GEMS (Gradient Echo Multi-Slice) sequence at a typical resolution of 256 × 128. Native and silica wet gels were fully solvent-exchanged with acetone and remained submerged in acetone for the duration of the experiment (typically 1–4 h). Empty capillary tubes were used in order to keep the orientation of the wet gel monoliths vertical. The images are transverse views at $z = 0$. Pixel density analysis was conducted using Adobe Photoshop 7.0.

For SEM, samples were coated with Au and the microscopy was conducted with a Hitachi S-4700 field-emission microscope. For nitrogen-adsorption porosimetry, samples were outgassed at 80 °C for 24 h and studies were conducted with an ASAP 2000 Surface Area/Pore Distribution analyzer (Micromeritics Instrument Corp.).

Three-point flexural bending tests were performed according to ASTM D790, Procedure A (Flexural Properties of Unreinforced and Reinforced Plastics and Electrical Insulating Materials), using an Instron 4469 universal testing machine frame with a 2 kN load cell (Instron part number 2525-818) and a three-point bend fixture, with 0.9 in. span and 25 mm roller diameter (Instron part number 2810-182). Typical samples were cylindrical, ~1 cm in diameter and ~4 cm in length. The crosshead speed was set at 0.04 in min^{-1}.

Dielectric characterization was conducted by measuring the capacitance of thin (~9 mm diameter, ~1 mm thick) and thick (~74 mm diameter, ~4 mm thick) crosslinked aerogel discs. The thin discs were cut from cylindrical monoliths with a diamond wafer blade (Hudson, Cleveland, OH) and saw (Isomet 11-1180, Low Speed Saw, Buehler Ltd., Evanston, IL) while the thick discs were prepared by molding. The lateral area of each disc was masked with duct tape and the top and bottom surfaces were sputter-coated with gold using a Baltek MED 20 Sputtering System. Copper wires were Scotch™-taped on the two surfaces, and were connected to an MFJ-259B SWR/RF analyzer (MFJ Enterprises, Inc., Mississippi State, MS), running in capacitance-measurement mode. Capacitance measurements were made at three different frequencies (72, 117 and 174 MHz) for the thin discs and at two different frequencies (8 and 25 MHz) for the thicker discs. The average capacitance values were corrected for fringe-field errors [12]. The relative dielectric constant ε_r of each sample was calculated using the corrected capacitance, area, and thickness of the samples. The precision of the dielectric constants was checked by comparing the ε_r value of thin discs with the value of a larger aerogel disc of the same composition and they were found to agree within experimental error (10%). The accuracy of the dielectric constant measurements was checked by measuring the dielectric constant of a known material, Plexiglas. The measured value was 2.2 ± 0.2, while the reported value is 2.55 ± 0.13 [13].

3. Results

3.1. Synthesis of isocyanate-crosslinked aerogel monoliths

Crosslinked aerogels are prepared by introducing and letting an isocyanate react with the mesoporous surfaces

of native silica wet gels, which were prepared either by a one-step base-catalyzed route or by a two-step process involving an acid-catalyzed sol and a base-catalyzed gel. Typical densities of one-step aerogels are in the range of 0.16–0.20 g cm^{-3}, and ~0.04–0.20 g cm^{-3} for two-step aerogels.

From a large array of available isocyanates, we have concentrated on Desmodur N3200, Desmodur N3300A, and Desmodur TDI. Desmodur N3200 and Desmodur N3300A are based on 1,6-hexamethylene diisocyanate (HDI). According to LC-MS analysis, the major component of N3200 has $m/z = 479.2$, with a 20% companion peak at 480.0 and major fragments at 453.7 (loss of CO) and at 311.3/285.4 (loss of HDI and subsequent loss of CO). On the basis of these results as well as on spectroscopic evidence (see Section 3.2.4), the major component of N3200 is

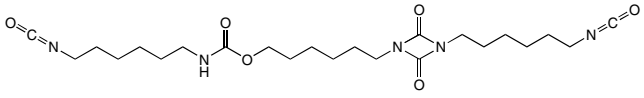

Desmodur N3200

Desmodur N3200 also contains another two linear components, [4] and a cluster of five long retention-time constituents, which all give fragments at $m/z = 504$, corresponding to the mass of the major component of N3300A.

Desmodur N3300A appears as a pure tri-isocyanate (see Section 3.2.4):

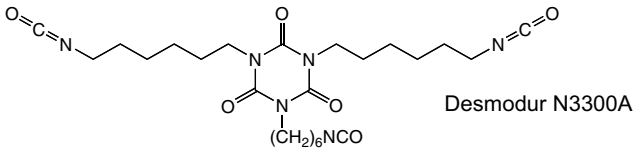

Desmodur N3300A

TDI is a mixture of aromatic diisocyanates based on toluene diisocyanate:

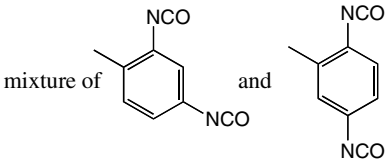

TDI

The three isocyanate monomers were introduced into the one-step wet gels, using either propylene carbonate or acetone. Propylene carbonate (bp 240 °C) allows crosslinking with wet gels either submerged in the isocyanate crosslinking solution or in closed containers with the crosslinking solution removed. The latter method facilitates better control of the extent of crosslinking because it precludes further diffusion and reaction of more isocyanate from the surrounding solution into the gel. However, propylene carbonate is a viscous solvent and wash cycles need to last longer to fully remove solvent prior to drying. Acetone solutions are less viscous and allow faster diffusion into and out of the mesopores thereby permitting substantially shorter wash cycles (e.g., 4 h per wash cycle, instead of 12 h). One disadvantage of using acetone, however, is that gels must remain submerged in the isocyanate solution during crosslinking resulting in denser crosslinked aerogels (e.g., 0.4–0.6 g cm^{-3}, starting from wet gels that would give aerogels with densities of ~0.18 g cm^{-3}). All crosslinking reaction mixtures develop pressure due to the evolution of CO_2 (identified by infrared absorption – see Section 2.5). As a final step, all wet gels are washed with acetone and dried with supercritical CO_2. An efficient all-acetone procedure involving one-step based-catalyzed gels crosslinked with Desmodur N3200 is summarized in Fig. 2. Finally, two-step gels can also be crosslinked in acetonitrile, i.e., the gelation solvent, and dried from acetonitrile/CO_2, thus eliminating several time-consuming solvent-exchange steps.

3.2. Characterization of isocyanate-crosslinked aerogel monoliths

Isocyanate-crosslinked aerogels were characterized macroscopically, microscopically and chemically.

3.2.1. Macroscopic characterization

As stated above, the density of crosslinked aerogels can be controlled by varying the concentration of the crosslinker in propylene carbonate. The relevant data thereon and photographs of crosslinked aerogels have been published previously [14]. Such aerogels appear translucent and are mechanically robust (see below). In order to 'look' inside crosslinked aerogel monoliths, we use NMR imaging 'cutting' across a geometric plane approximately through the middle of a native and a fully washed crosslinked wet gel, both submerged in acetone (Fig. 3). On the basis of dark pixel density analysis of the native silica wet gel relative to the background (see

[4] The second major linear component of N3200 gives molecular ion peak at 789.2 with satellites at 790.1 (50%), 791.1 (15%) and 792 (2%). The fragmentation pattern consists of pairs of peaks at 647.2/621.9 (1:0.9; loss of CO), 479.5/453.4 (1:0.9; loss of CO), and 311.3/285.4 (1:0.5; loss of CO). The third linear component of N3200 gives molecular ion at 815.3 with a satellite at 816 (40%) and a fragmentation pattern that includes peaks at 789.5 (loss of CO), 647.4/621.6 (1:0.4; loss of HDI and subsequent loss of CO), 479.4/453.5 (1:0.6; loss of 2 HDIs and subsequent loss of CO) and 311.3/285.4 (1:0.4; loss of 3 HDIs and subsequent loss of CO). On the basis of these data, the second major component of N3200 comprises an extension of its major component (shown in Section 3.1) by 2 HDIs, one linked through a diazetidinedione bridge and the other either through a carbamate bridge (molecular ion at 790) or a urea bridge (molecular ion at 789); the third major component of N3200 is also an extension of its major component by 2 HDIs, both linked through diazetidinedione bridges.

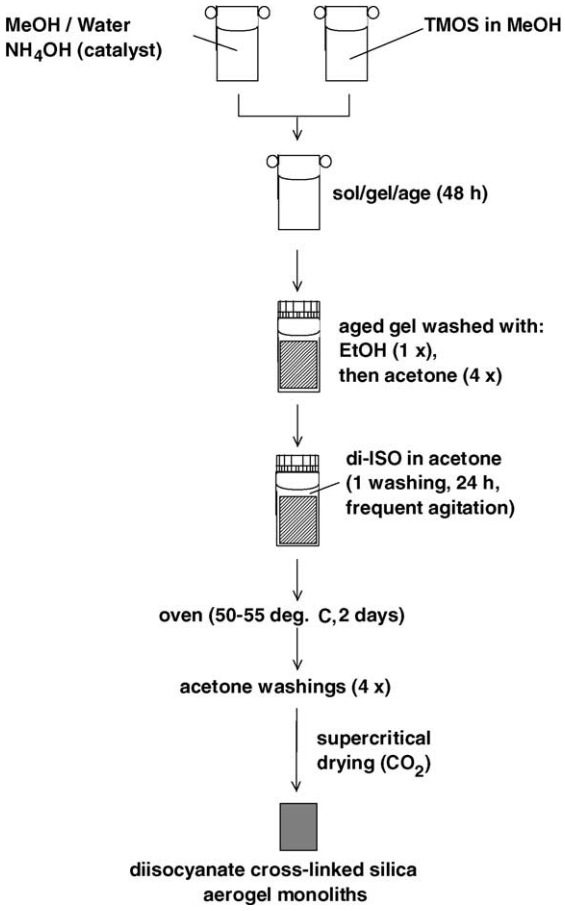

Fig. 2. A relatively rapid, all-acetone preparation procedure for isocyanate-crosslinked aerogels used in this study. Very recent results show that the aging step and all pre-crosslinking washes may be eliminated: newly formed wet gels can be put directly in the isocyanate solution and then directly into the oven. Washes after crosslinking are still necessary.

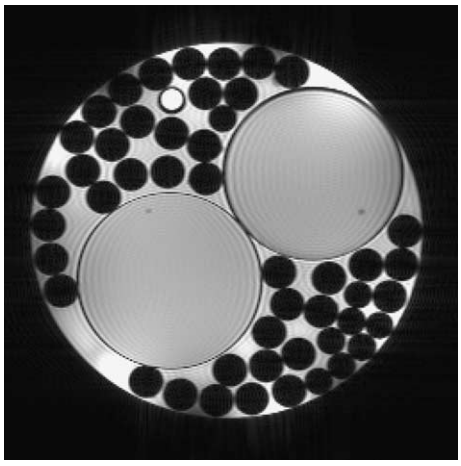

Fig. 3. Cross-sectional NMR image of a one-step base-catalyzed native silica wet gel monolith (lower left) and of a crosslinked one (upper right) in acetone. Dark circles: empty capillary tubes used to keep the monoliths straight up. Bright small circle: capillary tube filled with H_2O. Results of dark pixel density analysis (6 points per average). Native silica (bulk density of the resulting aerogel $\rho_b \sim 0.18\,g\,cm^{-3}$). Average near the perimeter: 160 ± 8; average around the center: 163 ± 1. Crosslinked silica ($\rho_b \sim 0.55\,g\,cm^{-3}$): Average near the perimeter: 152 ± 8; average around the center: 155 ± 1. Background average: 193 ± 10.

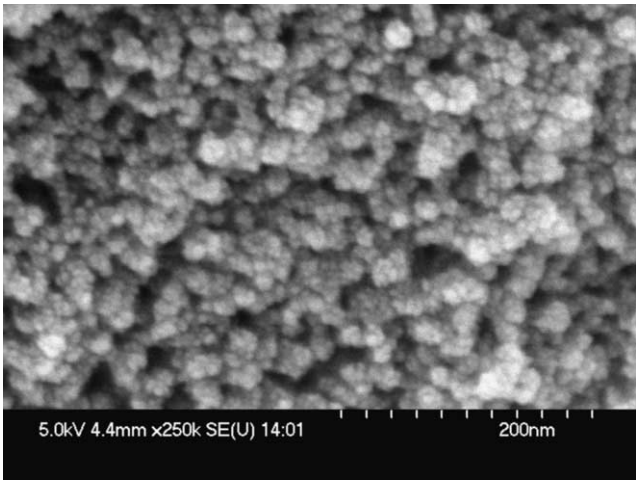

Fig. 4. Scanning electron microscopic imaging in the interior of a fractured crosslinked (N3200) silica aerogel monolith ($\rho_b = 0.38\,g\,cm^{-3}$).

Fig. 3, legend), the wet gel consists of $84 \pm 4\%$ of space filled with solvent. Since the primary structure consists of compact silica whose density is 1.7–2.2 $g\,cm^{-3}$ [5,15], it is calculated, based on the bulk density of the resulting aerogel ($\rho_b \sim 0.18\,g\,cm^{-3}$), that 89–92% v/v of the native silica wet gel of Fig. 3 consists of space filled with acetone. Since both NMR imaging and skeletal versus bulk density considerations yield similar results for the void space in the silica network, we conclude that NMR imaging is a reliable method for relative void space (porosity) analysis. Thus, based again on dark pixel density analysis, the NMR image of the crosslinked monolith of Fig. 3 is ~5% darker relative to the image of the native wet gel, and therefore it is calculated that the corresponding crosslinked aerogel ($\rho_b \sim 0.55\,g\,cm^{-3}$) consists of ~80–86% of void space.

3.2.2. Microscopic characterization

Under SEM examination of crosslinked aerogel samples (Fig. 4) we are still able to distinguish the same smallest (5–20 nm) features that are observed in the SEM of the native silica framework (refer to Fig. 1), confirming that new material has conformally coated the mesoporous surfaces. The Brunauer–Emmet–Teller (BET) surface-area analysis and average pore-diameter data (Table 1) show that as the density increases, the total surface area decreases while the average pore diameter initially increases.

3.2.3. Thermogravimetric characterization

Thermogravimetric analysis (TGA) was conducted from ambient temperature to 700 °C. One-step native

Table 1
Surface area and pore diameter data for native and crosslinked aerogels

Aerogel type	Crosslinker	Density ($g\,cm^{-3}$)	BET area ($m^2\,g^{-1}$)	Average pore diameter (nm)
One-step		0.180 ± 0.02	969 ± 30	13.8 ± 1
One-step	N3200[15a]	0.241 ± 0.003	324	
One-step	N3200[15a]	0.297 ± 0.007	308	18.1
One-step	N3200[15a]	0.390 ± 0.013	277 ± 30	22.1 ± 0.2
One-step	N3200[15a]	0.440 ± 0.016	197 ± 18	26.5 ± 3.3
One-step	N3200[15a]	0.447 ± 0.020	165	16.6
One-step	N3200[15a]	0.570 ± 0.020	150 ± 10	19.4 ± 0.6
One-step	N3300A	0.342 ± 0.014	248	12.4
One-step	N3300A	0.504 ± 0.034	186	17.7
One-step	N3300A	0.599 ± 0.040	142	14.0
One-step	N3300A	0.618 ± 0.005	140	10.6
One-step	TDI	0.242 ± 0.039	541	80.4
Two-step (15%, AC)[b]		0.085 ± 0.003	874	20.8
Two-step (15%, AN)[b]		0.087 ± 0.003	738	7.0
Two-step (8%, AC)[b]	N3200	0.129	222	8.6
Two-step (15%, AC)[b]	N3200	0.268 ± 0.004	228	7.6

[a] The crosslinker was Aldrich product No. 418005 (CAS No. 28182812), which has identical viscosity, and IR and ^{13}C-NMR spectra to Desmodur N3200.

[b] Processed and SCF-dried from the solvent indicated: AC, acetone; AN, acetonitrile. Percentages refer to the content (v/v) of the hydrolyzed TMOS stock solution in the sol (see Section 2).

silica aerogels lose ~4% of their weight up to 120 °C, and subsequently they gradually release another ~10% of their mass. Mass spectrometric analysis conducted in parallel to TGA shows that the early loss of mass is due mostly to acetone. Two-step gels, irrespective of density, lose ~10–12% of their mass below 100 °C (mostly acetone or acetonitrile) and gradually release another 3–5% of their mass to 700 °C. Infrared analysis conducted also in parallel to TGA shows gradual liberation of water from all gels, starting at ~100 °C. Importantly, including an additional wash step with pure water right after gelation yields aerogels that lose ~12% of their weight below 120 °C; by keeping such gels overnight under vacuum at room temperature, TGA analysis shows only an 8% loss of mass below 120 °C. These data demonstrate the ability of silica to retain adsorbed water throughout processing, all the way to the final aerogels. Aerogels crosslinked with N3200 or N3300A lose all of the crosslinker between 300 and 350 °C both in air and under nitrogen. For comparison, the onset of decomposition of polyurea derived from the reaction of N3300A with water is at ~300 °C in both nitrogen and air, while polyurea derived from the reaction of N3200 with water starts losing mass at ~250 °C in air, and at ~300 °C under nitrogen. For both kinds of polyurea, decomposition is complete by 500 °C.

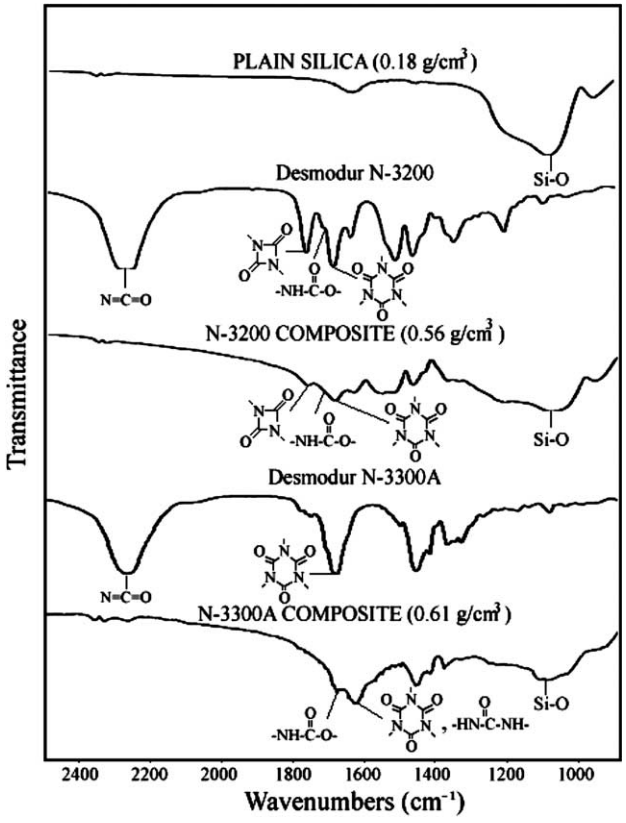

Fig. 5. Infrared analysis of silica, Desmodur N3200 isocyanate, Desmodur N3300A isocyanate, and of the corresponding crosslinked aerogels (N3200: $\rho_b = 0.56\,g\,cm^{-3}$; N3300A: $\rho_b = 0.61\,g\,cm^{-3}$).

3.2.4. Chemical characterization

Fig. 5 compares the infrared absorption data of aerogels crosslinked with N3200 and N3300A with the spectra of the corresponding monomers and with the spectrum of silica. As expected, the isocyanate stretch at ~2270 cm^{-1} is absent in the composites indicating that the isocyanate groups have completely reacted. The carbonyl stretch assigned to the diazetidinedione group of N3200 at 1767 cm^{-1} survives the crosslinking

conditions [16]. As expected, the isocyanurate ring carbonyl stretch at $\sim$1690 cm^{-1} is present in both N3200 and N3300A [17]. More importantly, the dominant carbonyl stretch in all silica-isocyanate composites is also at $\sim$1690 cm^{-1}. The presence of this band led us initially to think that crosslinking was based on the condensation of isocyanate groups into isocyanurate rings [14]. The ^{13}C-NMR evidence, however, indicates that the major structure of the polymeric crosslinker is polyurea, whose carbonyl vibrational band is also at $\sim$1690 cm^{-1} [18], and overlaps the isocyanurate carbonyl stretch.

Fig. 6 compares the carbonyl region of the ^{13}C-NMR spectrum of the composite with the same region for N3200 and of the reaction product between N3200 and methanol. Peak assignments are shown directly on the spectra. By reacting N3200 with methanol, the isocyanate carbon disappears. The new peak at $\sim$157 ppm is assigned to the formation of the terminal carbamates. Although the ^{13}C-NMR spectrum of the composite indicates formation of carbamate, the data are not very conclusive about the identity of the crosslinking polymer, because product peaks merge with the diazetidinedione resonance at 156–157 ppm [19].

Because the carbonyl region of the ^{13}C NMR of the N3300A composite is not complicated by the presence of diazetidinedione, this region is interpretationally more useful. As shown in Fig. 7(a), N3300A is a single component isocyanate, with a resonance at 121 ppm corresponding to the isocyanate carbonyl carbon and a second resonance at 148 ppm corresponding to the isocyanurate carbonyl carbon. [5] Upon reaction with methanol, the isocyanate group disappears and the new resonance band that appears at $\sim$157 ppm is assigned unambiguously to the newly formed carbamate groups (Fig. 7(b)). Upon reaction with isopropylamine, we obtain a solid product where the isocyanate group has reacted completely. The new resonance at $\sim$160 ppm is assigned to the newly formed urea groups (Fig. 7(c)) [20]. In an additional control experiment, the reaction of N3300A with water produces carbon dioxide and also yields a solid product with a new resonance at $\sim$160 ppm, corresponding to urea (Fig. 7(d)) [21]. The ^{13}C-NMR spectrum of the N3300A composite clearly shows the formation of both carbamate and urea and, importantly, the urea resonance dominates the spectrum (Fig. 7(e)). These results are independent of the process characteristics but further quantification of the relative amount of carbamate versus urea is not possible due to the severe peak overlap.

[5] The identity of the ^{13}C-NMR resonance of the isocyanurate carbonyl carbon was confirmed by comparison with the spectrum of commercially available triallyl-1,3.5-triazine-2,4,6(1*H*,3*H*,5*H*)-trione (Aldrich).

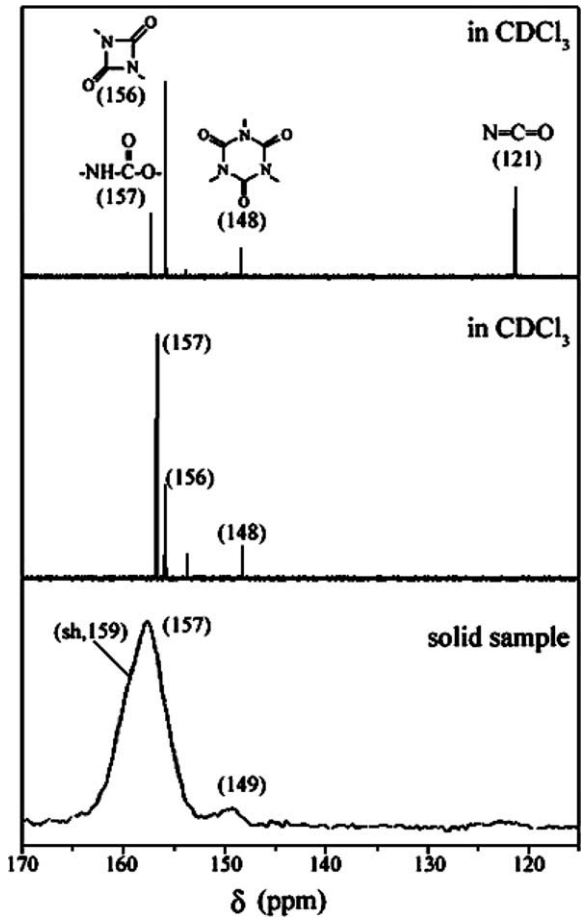

Fig. 6. Comparative ^{13}C-NMR characterization of the carbonyl region of: N3200 (top frame); the product of the reaction of N3200 and methanol (middle frame); and a N3200-crosslinked silica aerogel sample with $\rho_b \sim 0.55$ g cm^{-3} (bottom frame).

3.3. Selected physical properties of isocyanate-crosslinked aerogel monoliths

Both one- and two-step crosslinked silica aerogels were characterized for the two properties that have prevented broad practical applications of this class of materials, namely hydrophilicity and mechanical strength. Additionally, crosslinked aerogels were characterized for their dielectric constant, a property whose low value has been associated with the high porosity of aerogels.

3.3.1. Hydrophilicity of isocyanate-crosslinked silica aerogels

While hydrophilicity/hydrophobicity is usually determined through contact-angle measurements, the high porosity and the uptake of a water droplet by the mesopores render contact-angle measurements unreliable. Therefore, the hydrophilicity of native and crosslinked aerogels was tested by monitoring the relative water uptake from a water-vapor-saturated environment at room

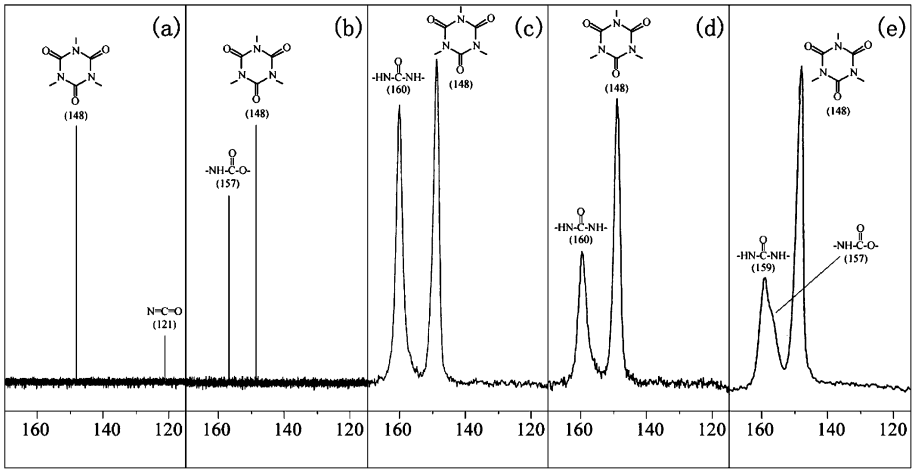

Fig. 7. Comparative ^{13}C-NMR characterization of the carbonyl region of: (a) N3300A ($CDCl_3$); (b) product of the reaction of N3300A and methanol ($CDCl_3$); (c) product of the reaction of N3300A and isopropylamine (solid sample); (d) product of the reaction of N3300A and water (solid sample); (e) N3300A-crosslinked aerogel with $\rho_b \sim 0.38\,g\,cm^{-3}$ (solid sample).

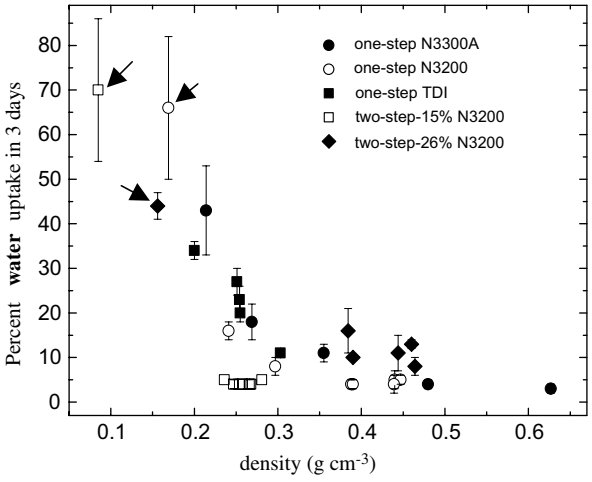

Fig. 8. Moisture uptake from a water-vapor-saturated environment of native and isocyanate-crosslinked silica aerogel monoliths. Error bars indicate the spread of the data (typically 3 points). Arrows point to native silica samples.

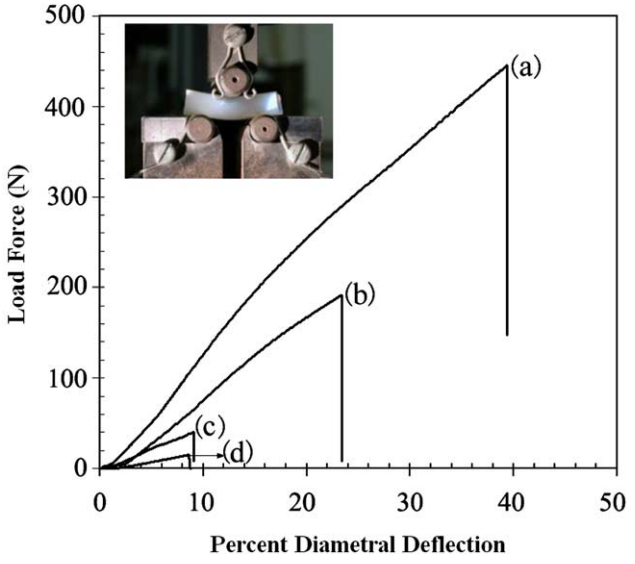

Fig. 9. Typical load force versus diametral deflection curves for three different N3300A-crosslinked silica aerogel monoliths. Curve (a): $\rho_b \sim 0.627\,g\,cm^{-3}$, diam. = 9.40 mm; Curve (b): $\rho_b \sim 0.481\,g\,cm^{-3}$, diam. = 9.75 mm; Curve (c): $\rho_b \sim 0.380\,g\,cm^{-3}$, diam. = 9.95 mm; Curve (d): $\rho_b \sim 0.276\,g\,cm^{-3}$, diam. = 10.05 mm.

temperature over a period of 3 d. The results are summarized in Fig. 8. Native silica aerogels take up 50–80% of their weight in water while the most dense crosslinked aerogels take up only 2–8% water, indicating that they are up to 10 times less hydrophilic. This behavior was independent of whether the underlying silica framework was prepared by either the one- or two-step process.

3.3.2. Mechanical testing of isocyanate-crosslinked silica aerogels

The strength and elastic modulus of one- and two-step aerogels at various stages of crosslinking (i.e., density) were tested by a short-beam three-point flexural bending method [22]. A primary concern was to ensure that all samples were tested under identical conditions for internal consistency. Fig. 9 shows typical load force versus diametral deflection curves for three different one-step aerogel monoliths (underlying bulk silica density $\sim 0.18\,g\,cm^{-3}$ s) crosslinked with Desmodur N3300A. The modulus of elasticity, E, is calculated from the slope, S, of the linear part of the load-deformation curves using Eq. (2), where L is the span and r the radius of the aerogel monolith [14].

$$E = \frac{SL^3}{12\pi r^4}. \tag{2}$$

The strength and modulus data for a variety of native and crosslinked aerogels are summarized in Fig. 10.

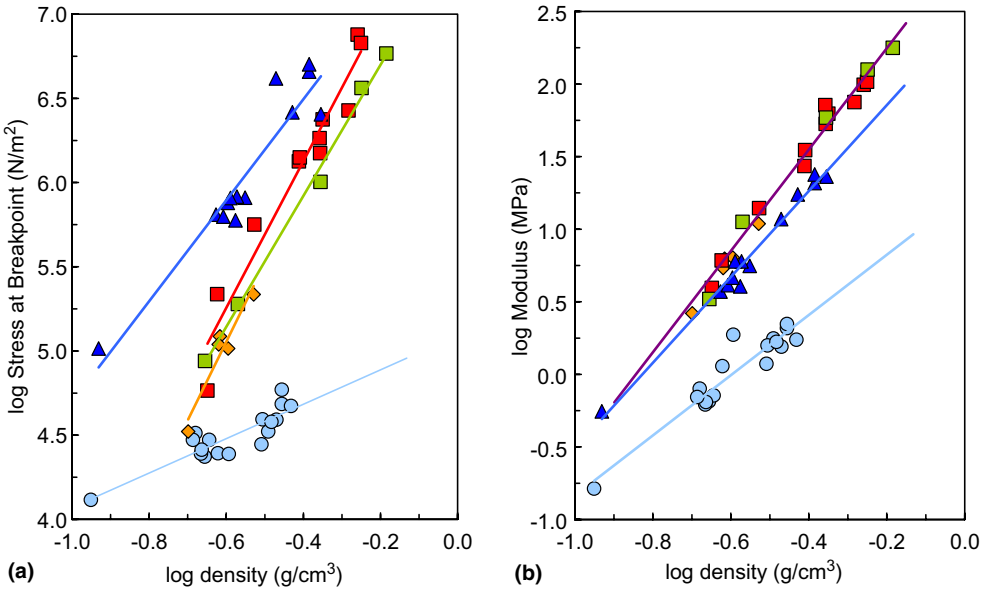

Fig. 10. Mechanical properties of isocyanate-crosslinked silica aerogels. (a) Strength versus density: ○ native silica aerogels: slope = 1.03; intercept = 5.09; $R^2 = 0.770$. ■ one-step crosslinked with N3200; slope = 4.40; intercept = 7.87; $R^2 = 0.940$. ■ one-step crosslinked with N3300A; slope = 4.65; intercept = 7.84; $R^2 = 0.920$. ◆ one-step crosslinked with TDI; slope = 3.89; intercept = 7.48; $R^2 = 0.995$. ▲ two-step aerogels crosslinked with N3200; slope = 3.00; intercept = 7.695; $R^2 = 0.897$. (b) Modulus versus density: Purple line (■, ■, ◆) slope = 3.99; intercept = 2.94; $R^2 = 0.98$. Light blue line (○) slope = 2.07; intercept = 1.24; $R^2 = 0.90$. Dark blue line (▲) slope = 2.96; intercept = 2.45; $R^2 = 0.98$. The bulk density, ρ_b, of the underlying silica framework was ~0.18 g cm^{-3} for the one-step aerogels and ~0.085 g cm^{-3} for the two-step aerogels. (For interpretation of color in this figure, the reader is referred to the web version of this article.)

3.3.3. Dielectric testing of isocyanate-crosslinked silica aerogels

An ideal insulator for fast electronics requires a relative dielectric constant close to that of air ($\varepsilon_{air} = 1$). Aerogels, which consist of >90% space filled with air, have an estimated relative dielectric constant in the range of 1–2 and, therefore, are ideal materials for such applications. As a result of their fragility, however, processing is almost impossible. Isocyanate-crosslinked aerogels can be machined, but the question is whether the increase in density that accompanies the increase in strength and makes these materials processible, compromises the dielectric properties. For this reason, discs were cut from different crosslinked monoliths and the capacitance was measured as described in Section 2.5.

From the radius-to-thickness ratio of each sample, the capacitance values were corrected for fringe-field effects in air using Eq. (3) [12], where x is the radius-to-thickness ratio of the disk.

$$\frac{C_{measured}}{C_{simple}} = 1 + \frac{2}{\pi x}\ln\left(\frac{8\pi x}{e}\right) + \left(\frac{1}{\pi x}\ln\left(\frac{1}{8\pi x}\right)\right)^2. \quad (3)$$

The relative dielectric constant ε_r was calculated using the corrected capacitance, area, and thickness of the samples using Eq. (4):

$$C_{simple} = \frac{\varepsilon_0 \varepsilon_r \pi R^2}{d}. \quad (4)$$

For example, the capacitance of a larger N3200-crosslinked disk ($\rho_b = 0.56$ g cm^{-3}, thickness = 3.90 mm, diameter = 74.8 mm) was 32 and 34 pF at 8 and 25 MHz, respectively. The average capacitance, corrected for the capacitance of the connecting wires (6 pF) and the fringe-field effects (Eq. (2)) was 20 ± 1 pF. The relative dielectric constant ε_r calculated from this value is 2.0 ± 0.1. The dielectric constants for all samples tested are provided in Table 2.

Table 2
Experimental dielectric constants, ε_r, for typical crosslinked silica aerogel monoliths derived by a one-step base-catalyzed route[a]

Crosslinker	Density (g m^{-3})	ε_r (number of samples)
N3300A	0.480 ± 0.001	1.4 ± 0.4 (2)
N3300A	0.627 ± 0.012	1.9 ± 0.1 (2)
N3200	0.522 ± 0.046	1.8 ± 0.1 (2)
N3200	0.564 ± 0.042	1.9 ± 0.2 (2)
N3200	0.562 ± 0.087	2.2 ± 0.2 (3)
N3200	0.501 ± 0.087	1.9 ± 0.2 (3)

[a] All samples rely on a silica framework with bulk density of ~0.18 g cm^{-3}.

4. Discussion

4.1. Chemical characterization and the mechanism of crosslinking

Di- or tri-isocyanates are used commercially for application as coatings, which are hardened (cured) by the moisture in the air. For such applications the vapor

pressure of the isocyanate itself must be kept low. Such higher viscosity/lower vapor pressure isocyanates can be made either by catalytic condensation of lower molecular weight diisocyanates [19], for example with hexamethylene diisocyanate (HDI), or by direct synthesis, as for example via the base-catalyzed ring closure of the condensation product of a *N*,*N*′-dialkylurea and phosgene [16]. Because the isocyanurate system is thermodynamically more stable than diazetidinedione [19], it is easier to prepare it selectively. In that regard, it is not surprising that N3300A appears as a single-component reagent, while N3200 is a mixture that includes diazetidinediones, isocyanuates and carbamates. And although it is known that the diazetidinedione system may open up under certain conditions [23], for example in the tri-*n*-butylphosphine-catalyzed reaction with amines to yield ureas, it seems to survive during crosslinking of silica and during our control experiments.

The spectroscopic data and particularly the results from ^{13}C-NMR, taken with the fact that crosslinking is accompanied by the evolution of carbon dioxide, lead to the conclusion that the crosslinking mechanism is as shown in Fig. 11. In brief, crosslinking silica aerogels with isocyanates involves reaction of the isocyanate both with the surface of silica and with itself via a reagent (water) that is confined onto the surface of silica, and results in the formation of polyurethane and polyurea. We note that the reaction of the isocyanate with ≡SiOH groups appears to be much faster than hydrolysis and condensation to urea: introduction of isocyanate into the sol of either the one-step or the two-step process prevents gelation completely, presumably by fast reaction with and consumption of the hydroxyl functionality. Furthermore, although in general the solvents used in the crosslinking process were not anhydrous, the water involved in the crosslinking reaction originates from the water used for hydrolysis of TMOS and gelation; this conclusion is confirmed by a control experiment where heating the crosslinking solution by itself, without a gel in it, does not produce detectable amounts of CO_2 (see Section 2.5). It is still possible that silica, due to its hydrophilic nature, extracts water from the solvent and the resulting local high concentration of water at the surface accelerates the bimolecular reactions involved in crosslinking. This hypothesis was tested by varying the amount of water during gelation of two-step gels with a subsequent evaluation of the ability of the resulting wet gels to crosslink: decreasing the amount of water used to prepare a 15% gel (see Section 2.2), even by a factor of 10, did not prevent gelation, but the resulting wet gels could not be crosslinked.

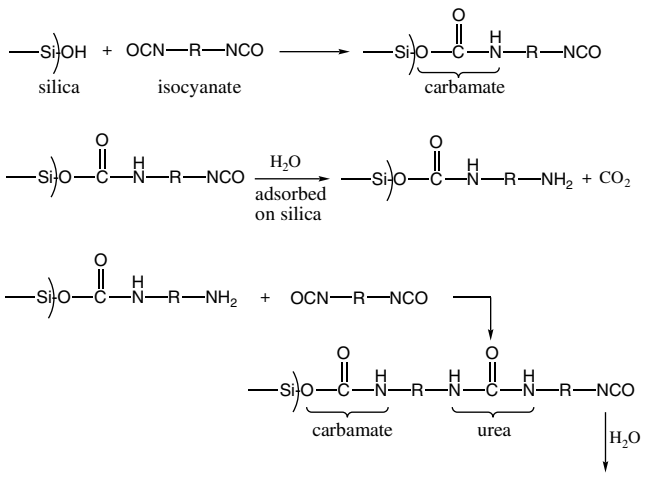

Fig. 11. Proposed mechanism for crosslinking silica with isocyanates.

4.2. Structural characterization

The NMR imaging indicates that crosslinked aerogels still consist of mostly empty space, despite the up to threefold increase in density compared with the underlying silica framework. [6] To reconcile this fact with the nitrogen-adsorption data, which show a significant decrease in surface area and an initial increase in average pore diameter (Table 1), we are forced to conclude that the first monolayer of the polymer blocks access to the micropores leading to the primary particles. Thus, considering the BET surface area of our base-catalyzed native silica aerogels ($\sim$970 m^2 g^{-1}) and the molecular formula of the crosslinker, the total BET surface area coverage of a N3200-crosslinked aerogel with a density of $\sim$0.55 g cm^{-3} corresponds to 4.8 monolayers. (Note: this calculation does not include a shrinkage correction and assumes that N3200 is a single component monomer and that the first monolayer is based on condensation to urethane while the subsequent layers involve fragmentation and condensation to polyurea.) Since the first several layers of monomolecular polymer probably block channels that lead to micropores, thus inhibiting further crosslinking in those pores, the actual coverage of the mesoporous surfaces should be at least double the calculated value. We also note that the polymer may lay flat on the particles; in other words, the calculated number of 'monolayers' may just represent the average length of the tethers that bridge the nanoparticles, rather than a layer-by-layer accumulation of polymer.

[6] It should be pointed out that in response to a reviewer's comment, preliminary attenuated total reflectance infrared data across 1 cm diam. crosslinked aerogel disks indicate a variation in the amount of polymer from the perimeter to the center. This radial variation can be as high as 30%, depending on whether crosslinking was carried out in an isocyanate solution, and reflects the fact that fresh isocyanate diffuses in from the bulk. One promising alternative that is currently under investigation with low-boiling solvents (acetone, acetonitrile) is to carry out crosslinking of isocyanate-equilibrated wet gels in isocyanate-free solvents.

4.3. Physical properties (hydrophilicity, mechanical strength, dielectric constant)

Practical application of aerogels has been slow owing to their hydrophilicity and fragility. Hydrophilicity reduces the environmental stability of silica aerogels. Water absorbed onto the surfaces of the mesopores provides the —H and —OH groups needed to satisfy the unsaturation generated by cleavage of the —Si—O—Si— bridges during fracture. Although isocyanate-crosslinked silica aerogels do not collapse when placed in contact with water, the pores take up water, and the gels sink. Isocyanate-crosslinked aerogels are therefore not hydrophobic, but they are much less hydrophilic than native silica (see Fig. 8).

As shown in Fig. 9, crosslinked aerogels are also mechanically strong. According to these data, stronger aerogels (i.e., aerogels requiring more force to break) are also stiffer (i.e., they take more force to bend) and tougher (i.e., they can store more energy, as judged by the larger area under the stress–deflection curves). Although power-law dependences between strength and density, and between modulus and density of native silica aerogels, such as those shown in Fig. 10, are known [24,25], several important observations can be made concerning these data. First, at equivalent densities crosslinked aerogels exhibit greater strength than the native gels. Second, increasing density increases strength for all types of aerogels. However, strength increases more rapidly with density by adding polymer than by adding silica. One explanation is that while a denser silica network has a higher interparticle connectivity, this approach is apparently not as efficient a method to increase strength as increasing the width of the necks between secondary particles through the conformal addition of polymer to the surface of the network. In this context, it is noted that aging silica wet gels results in dissolution and re-precipitation, preferentially at the neck areas, rendering them also wider. This process increases the strength of silica only by a factor of ~2, probably because it is limited by the fact that the dissolution process renders the silica framework weaker [26]. Finally, the skeletal morphology of the inorganic network appears to play an important role in the distribution of the load forces. For one-step base-catalyzed silica, all three isocyanates in this study give similar results in terms of strength and identical results in terms of stiffness; however, when the silica framework is derived from the two-step process, both strength and modulus show a different sensitivity towards density variation, implying that the inorganic network affects the overall behavior of the resulting aerogel. In this context, we are currently investigating the properties of isocyanate-crosslinked aerogels based on alumina, titania, zirconia, and other metal oxides.

Clearly, crosslinking decreases hydrophilicity and increases strength. The question, however, is whether and how those changes affect desirable properties closely related to the high void volume (porosity) of aerogels.

Experimental values for one such property, the dielectric constant of isocyanate-crosslinked aerogels, are closer to the value reported for native silica aerogels (equal to 1.48 for silica with porosity equal to 86%, [27]), than to the dielectric constant of polyurethane (in the range 4–5 [28]), or of dense silica (~4.2 [29]). Although the densities of the crosslinked samples that were tested for their dielectric properties are considerably higher than what one would have expected intuitively from the relatively small increase in the dielectric constant, our dielectric results indicate that the void mesoporous space has not been compromised significantly by crosslinking. This assessment is in agreement with the NMR imaging data. In order to reconcile the fact that crosslinked monoliths shrink by 10–12% relative to native silica [14] with the fact that mesoporosity is maintained, we conclude that polymerization of the crosslinker compresses the underlying secondary particles by an equivalent amount.

5. Conclusions

This study has shown that polymerization of isocyanates templated to the surface of a silica network reinforces aerogels by a factor of ~300 with a much smaller increase in density by only a factor of ~3. This process has been referred to as crosslinking and the underlying mechanism has been traced to reactions of the isocyanate (i.e., the crosslinker) first with the surface of the silica and then with itself via a process involving water adsorbed on the mesoporous surfaces. This mechanism implies that other types of aerogels (e.g., alumina, titania, zirconia, etc.) could also be crosslinked, not only with isocyanates but also with other types of crosslinkers (e.g., epoxies, polyolefins, polyimides) provided that the crosslinker is able to react both with the mesoporous surface of the inorganic framework, and also with itself via a reaction with a reagent or a catalyst confined at or near that surface.

Acknowledgments

Financial support from NASA Glenn Research Center Director's Discretionary Fund (DDF) is gratefully acknowledged. We thank Dr Steven Jones of JPL for useful discussions concerning the two-step gelation process, and Bayer Corporation for the generous supply of isocyanates.

References

[1] For example refer to the thematic issue on 'Issues in Nanotechnology' in Science Magazine, 24 November 2000.
[2] A.M. Thayer, Chem. Eng. News 1 (September) (2003) 15.
[3] D.R. Rolison, Science 299 (2003) 1698.
[4] C.J. Brinker, G.W. Scherer, Sol–gel Science; The Physics and Chemistry of Sol–gel Processing, Academic, New York, 1990.
[5] N. Hüsing, U. Schubert, Angew. Chem. Int. Ed. 37 (1998) 22.
[6] J. Fricke, Sci. Am. (May) (1988) 92.
[7] A.C. Pierre, G.M. Pajonk, Chem. Rev. 102 (2002) 4243.
[8] C.A. Morris, M.L. Anderson, R.M. Stroud, C.I. Merzbacher, D.R. Rolison, Science 284 (1999) 622.
[9] Z.W. Wicks Jr., F.N. Jones, S.P. Pappas, Organic Coatings: Science and Technology, vol. 1, Wiley, New York, 1992, pp. 188–211 (Chapter 12).
[10] N. Leventis, I.A. Elder, D.R. Rolison, M.L. Anderson, C.I. Merzbacher, Chem. Mater. 11 (1999) 2837.
[11] T.M. Tillotson, L.W. Hrubesh, J. Non-Cryst. Solids 145 (1992) 44.
[12] G.J. Sloggett, N.G. Barton, S.J. Spencer, J. Phys. A: Math. Gen. 19 (1986) 2725.
[13] A. Reza, IEEE Trans. Microwave Theor. Techn. 46 (1998) 1307.
[14] N. Leventis, C. Sotiriou-Leventis, G. Zhang, A.-M.M. Rawashdeh, Nano Lett. 2 (2002) 957.
[15] J. Fricke, J. Non-Cryst. Solids 100 (1988) 169.
[16] D.K. White, F.D. Greene, J. Org. Chem. 43 (1978) 4530.
[17] R.B. Wilson, Y.-S. Chen, I.C. Paul, D.Y. Curtin, J. Am. Chem. Soc. 105 (1983) 1672.
[18] X.F. Yang, C. Vang, D.E. Tallman, G.P. Bierwagen, S.G. Croll, S. Rohlik, Polym. Degr. Stabil. 74 (2001) 341.
[19] F.U. Richter, J. Schmitz, H.-J. Laas, R. Halpaap, Polym. Prepr. 44 (2003) 46.
[20] H.-L. Wang, H.-M. Kao, M. Digar, T.-C. Wen, Macromolecules 34 (2001) 529.
[21] H. Ni, D.J. Aaserud, W.J. Simonsick Jr., M.D. Soucek, Polymer 41 (2000) 57.
[22] J.M. Gere, S.P. Timoshenko, Mechanics of Materials, fourth ed., PWS Publishing, Boston, 1997.
[23] N. Risch, U. Westerwelle, J. Kiene, R. Keuper, J. Prakt. Chem. 341 (1999) 616.
[24] T. Woignier, J. Reynes, A. Hafidi Alaoui, I. Beurroies, J. Phalippou, J. Non-Cryst. Solids 241 (1998) 45.
[25] T. Woignier, J. Phalippou, Rev. Phys. Appl. 24 (1989) 179.
[26] S. Hæreid, J. Anderson, M.-A. Einarsrud, D.W. Hua, D.M. Smith, J. Non-Cryst. Solids 185 (1995) 221.
[27] L.W. Hrubesh, J.F. Poco, J. Non-Cryst. Solids 188 (1995) 46.
[28] P. Pisis, G. Georgoussis, V.A. Bershtein, E. Neagu, A.M. Fainleib, J. Non-Cryst. Solids 305 (2002) 150.
[29] K. Maex, M.R. Baklanov, D. Shamiryan, F. Iacopi, S.H. Brongersma, Z.S. Yanovitskaya, J. Appl. Phys. 93 (2003) 8793.